NAVAL POSTGRADUATE SCHOOL

Monterey, California

THESIS

**DESIGN AND ANALYSIS OF THE LAUNCH
VEHICLE ADAPTER FITTING FOR THE PETITE
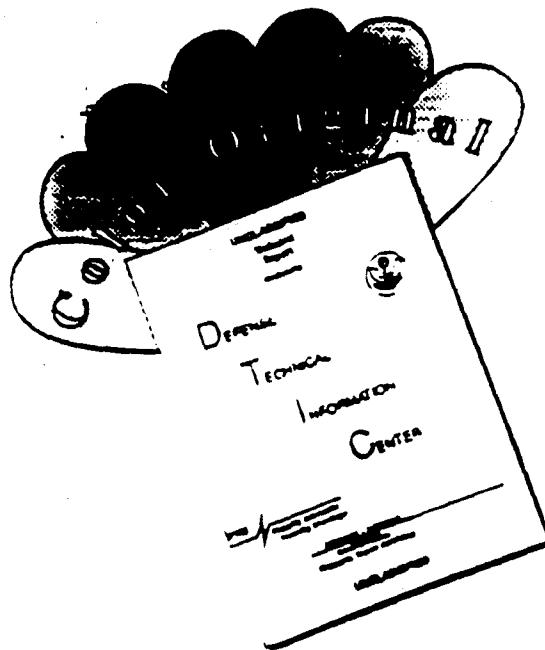AMATEUR NAVY SATELLITE (PANSAT)**

by

Brian Bernard Gannon

September 1994

Thesis Advisor: Sandi Scrivener

19950112 000

DISCLAIMER NOTICE

THIS DOCUMENT IS BEST QUALITY AVAILABLE. THE COPY FURNISHED TO DTIC CONTAINED A SIGNIFICANT NUMBER OF COLOR PAGES WHICH DO NOT REPRODUCE LEGIBLY ON BLACK AND WHITE MICROFICHE.

REPORT DOCUMENTATION PAGE			Form Approved OMB No. 0704
Public reporting burden for this collection of information is estimated to average 1 hour per response, including the time for reviewing instruction, searching existing data sources, gathering and maintaining the data needed, and completing and reviewing the collection of information. Send comments regarding this burden estimate or any other aspect of this collection of information, including suggestions for reducing this burden, to Washington headquarters Services, Directorate for Information Operations and Reports, 1215 Jefferson Davis Highway, Suite 1204, Arlington, VA 22202-4302, and to the Office of Management and Budget, Paperwork Reduction Project (0704-0188) Washington DC 20503.			
1. AGENCY USE ONLY *(Leave blank)*	2. REPORT DATE September 1994	3. REPORT TYPE AND DATES COVERED Master's Thesis	
4. TITLE AND SUBTITLE DESIGN AND ANALYSIS OF THE LAUNCH VEHICLE ADAPTER FITTING FOR THE PETITE AMATEUR NAVY SATELLITE (PANSAT) (U)		5. FUNDING NUMBERS	
6. AUTHOR(S) Gannon, Brian B.			
7. PERFORMING ORGANIZATION NAME(S) AND ADDRESS(ES) Naval Postgraduate School Monterey CA 93943-5000		8. PERFORMING ORGANIZATION REPORT NUMBER	
9. SPONSORING/MONITORING AGENCY NAME(S) AND ADDRESS(ES)		10. SPONSORING/MONITORING AGENCY REPORT NUMBER	
11. SUPPLEMENTARY NOTES The views expressed in this thesis are those of the author and do not reflect the official policy or position of the Department of Defense or the U.S. Government.			
12a. DISTRIBUTION/AVAILABILITY STATEMENT Approved for public release; distribution unlimited		12b. DISTRIBUTION CODE	
13. ABSTRACT *(maximum 200 words)* The Petite Amateur Navy Satellite (PANSAT) is a small communications satellite being developed at the Naval Postgraduate School. This thesis provides a structural design and analysis for the adapter fitting which mates PANSAT to the space shuttle Get Away Special (GAS) cannister launching system. Launch vehicle loading and interface requirements were combined with PANSAT design priorities to determine design specifications. Structural Dynamics Research Corporation's I-DEAS Masters Series software was utilized to model two adapter designs. The finite element solver in I-DEAS was used to analyze the two designs for strength and natural frequency. Design and analysis of fasteners, used to attach the adapter fitting to PANSAT, were also conducted. The results showed that a titanium alloy adapter, which does not shadow the solar arrays, and stainless steel fasteners exceeded all design specifications.			
14. SUBJECT TERMS Adapter fitting, PANSAT, finite element analysis, fastener analysis, structural design		15. NUMBER OF PAGES 53	
		16. PRICE CODE	
17. SECURITY CLASSIFICATION OF REPORT Unclassified	18. SECURITY CLASSIFICATION OF THIS PAGE Unclassified	19. SECURITY CLASSIFICATION OF ABSTRACT Unclassified	20. LIMITATION OF ABSTRACT UL

NSN 7540-01-280-5500

Standard Form 298 (Rev. 2-89)
Prescribed by ANSI Std. 239-18

DTIC QUALITY INSPECTED 3

i

.

DESIGN AND ANALYSIS OF THE LAUNCH VEHICLE ADAPTER FITTING FOR THE PETITE AMATEUR NAVY SATELLITE (PANSAT)

Brian B. Gannon
Lieutenant, United States Navy
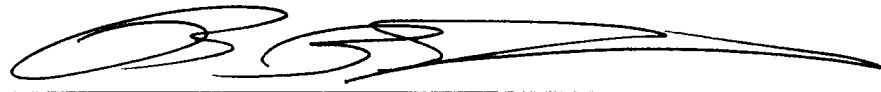B.S., Illinois Institute of Technology, 1985

Submitted in partial fulfillment of the
requirements for the degree of

MASTER OF SCIENCE IN ASTRONAUTICAL ENGINEERING

from the

NAVAL POSTGRADUATE SCHOOL
September 1994
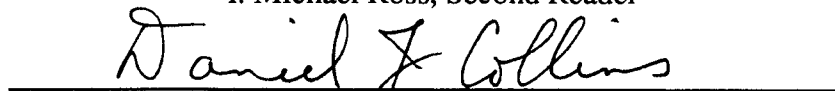
Author: _____
Brian B. Gannon

Approved by: _____
Sandra L. Scrivener, Thesis Advisor

_____
I. Michael Ross, Second Reader

_____
Daniel J. Collins, Chairman
Department of Aeronautics and Astronautics

iii

iv

ABSTRACT

The Petite Amateur Navy Satellite (PANSAT) is a small communications satellite being developed at the Naval Postgraduate School. This thesis provides a structural design and analysis for the adapter fitting which mates PANSAT to the space shuttle Get Away Special (GAS) cannister launching system. Launch vehicle loading and interface requirements were combined with PANSAT design priorities to determine design specifications. Structural Dynamics Research Corporation's I-DEAS Masters Series software was utilized to model two adapter designs. The finite element solver in I-DEAS was used to analyze the two designs for strength and natural frequency. Design and analysis of fasteners, used to attach the adapter fitting to PANSAT, were also conducted. The results showed that a titanium alloy adapter, which does not shadow the solar arrays, and stainless steel fasteners exceeded all design specifications.

TABLE OF CONTENTS

I. INTRODUCTION

A. PANSAT MISSION

The Naval Postgraduate School (NPS) is developing the Petite Amateur Navy Satellite (PANSAT), a small satellite for digital communication within the amateur frequency band. PANSAT is designed to be a direct sequence spread spectrum communications satellite with store and forward capabilities. PANSAT will be utilized by the students at NPS for experimentation in digital communications and by amateur radio enthusiasts.

The overall design priorites for PANSAT are to keep the costs low, simplify the design as much as possible, and have good reliability. The satellite consists of eighteen 7.125 inch by 7.125 inch panels and eight equilateral triangle panels arranged in a "stop sign" pattern when viewed from any side. Figure 1 shows the main structure of PANSAT.
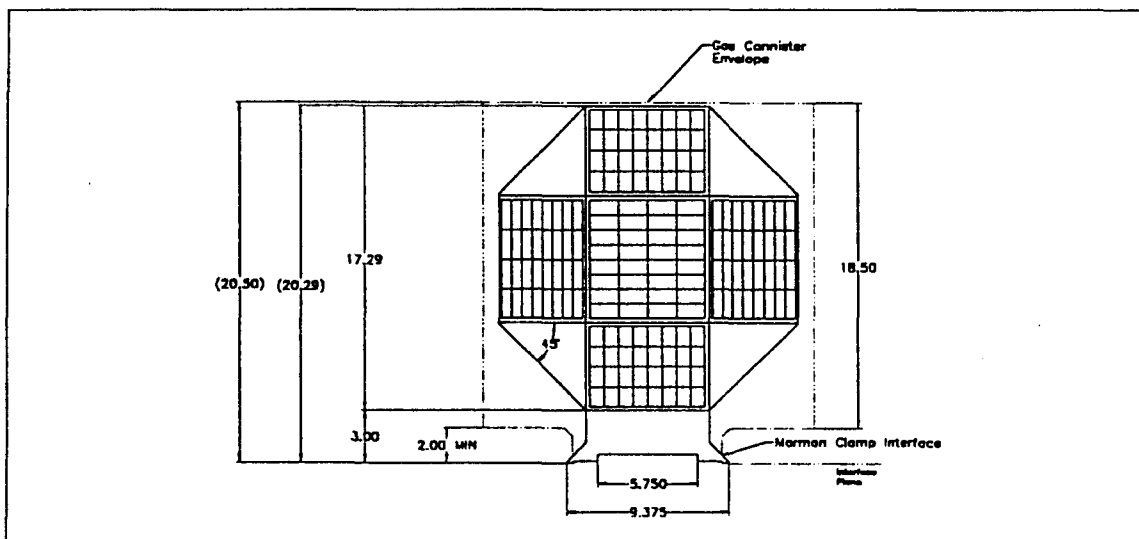

Figure 1. PANSAT Main Structure [Ref 1].

The maximum diameter is 18.62 inches and maximum weight is 150 lbf. The main structure is constructed of 6061-T6 aluminum due to its low cost, good machineability, and its ability to withstand the relatively low loading seen during launch. Power is generated by silicon based solar cells distributed over the surface of the satellite while power storage is provided by nickle-cadmium batteries. The spacecraft utilizes no attitude control or propulsion systems in order to simplify the design and reduce cost. This will cause the spacecraft to tumble in its orbit and drives the design and placement of the solar arrays. Communications are provided by four omni-directional antennas mounted on the exterior structure. The operating frequency is centered at 436.5 Mhz with a spread of 2.5 Mhz. Data transmission will occur at a bit rate of 9600 bps with up to 4 MB of storage onboard.

B.   ORBIT INJECTION

Launch of PANSAT will be accomplished via the Space Shuttle Hitchhiker program. The Space Shuttle Hitchhiker program was chosen due to the design constraints imposed by the Shuttle Self-Contained Payload (SSCP) program and significantly lower cost of launch when compared to dedicated expendable launch vehicles. The design constraints imposed by the SSCP program will allow easier qualification for other launch vehicles if desired. Since Hitchhiker payloads are considered secondary payloads, PANSAT will have to accept the orbital parameters required by the primary payload of the shuttle launch. The current launch window is scheduled for shuttle mission STS-83, launching in December 1996. This shuttle mission will orbit at 394.5 km altitude and 51.6 deg of inclination, providing approximately 6 minutes of coverage for communications between the satellite and NPS. The satellite will be deployed from a Get Away Special (GAS) canister mounted in the shuttle cargo bay as shown in Figure 2.
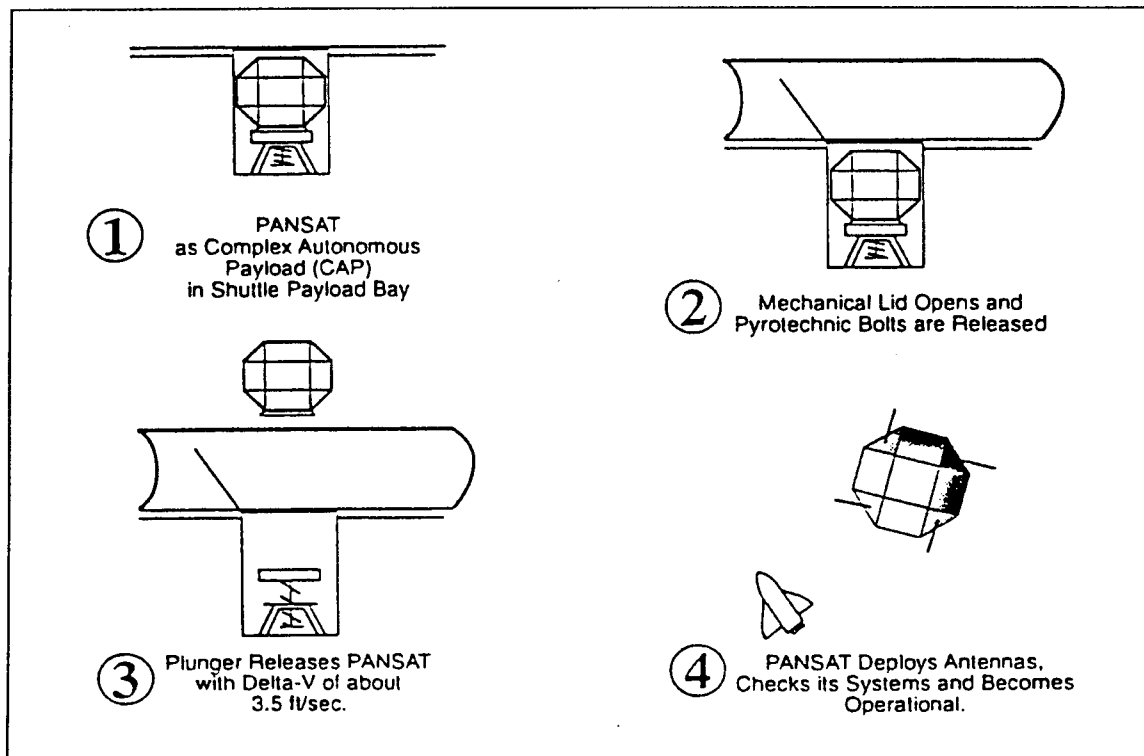
Figure 2. PANSAT Launch Sequence [Ref. 2].

The standard GAS canister is basically a cylindrical can, sealed at both ends that is used to contain autonomous experiments flown on shuttle missions. The canister is mounted in the shuttle payload bay to the longerons running along the sides of the bay. The standard GAS canister does not contain a motorized door assembly or an ejection mechanism both of which are required by PANSAT. The motorized door assembly allows the canister to open to space. The ejection mechanism consists of a pedestal, a Marman clamp to hold the satellite to the pedestal during shuttle launch and a spring loaded plunger mechanism to eject free-flier experiments into space at 3.5 fps. Therefore a GAS canister modified as a free-flier experiment will be used for PANSAT. This will designate PANSAT as a Complex Autonomous Payload (CAP) and result in a different queuing process than standard GAS payloads for launch. The GAS canister assembly is shown in Figure 3.

3
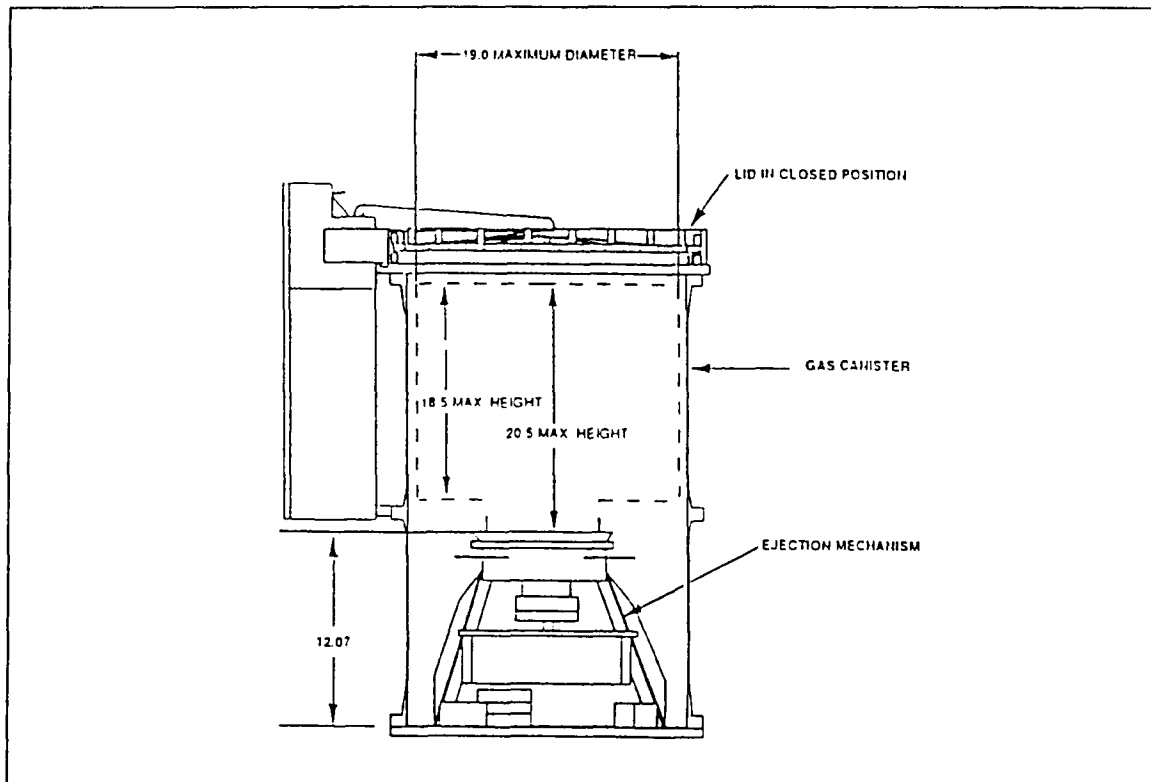
Figure 3. Modified GAS Canister [Ref. 3].

The adapter fitting, discussed in this thesis, mates the structure of PANSAT to the ejection mechanism of the GAS canister. The adapter must meet all envelope requirements of the ejection mechanism as well as those of PANSAT. The design of the adapter must be robust enough to survive the worst case launch loading at maximum satellite mass and stiff enough not to couple with the natural frequency of the shuttle. The following chapters will discuss the requirements, design, and analysis of the adapter fitting. Chapter II discusses the launch vehicle environment, limit loading, frequency requirements and adapter envelope. Chapter III provides an overview of the computer software used to model and analyze the adapter. Chapter IV details design options while Chapter V presents the analysis results. Chapter VI presents the conclusions and recommendations for the design employed.

4

II. LAUNCH VEHICLE REQUIREMENTS

The SSCP program design requirements are quite high and lead to a very conservative design. This is due to the overriding safety concerns of manned missions. The requirements for a payload under the SSCP program are numerous, however only those affecting the adapter design will be discussed here. [Ref. 4]

A. PAYLOAD REQUIREMENTS

The payload has several requirements to meet so it does not exceed the limitations of the free-flier modified GAS canister. The payload cannot exceed 150 lbf maximum weight, 19.0 inches maximum diameter, and 18.5 inches maximum height. The center of mass of the payload must be within 0.5 inches of the canister centerline and cannot exceed 10.25 inches above the separation plane of the Marman clamp interface. The actual height specification limit for the center of mass was not confirmed by NASA at the time of this thesis. The payload weight used in the adapter design was 150 lbf. The center of mass was not accurately known at the time of this thesis. Utilizing the geometric center of the payload resulted in a center of mass on the centerline of the GAS canister but 10.60 inches above the Marman clamp interface plane. This excess over the 10.25 inch requirement was kept in the analysis and results in a slightly more severe loading condition on the adapter than would otherwise be seen. Although this center of mass height is technically over the specification, the more severe loading condition created increases the safety margin of the adapter and thus does not invalidate the design.

B. LAUNCH LOADING

PANSAT must be able to survive the worst case loading during shuttle launch, ejection from the GAS canister, and possible landing in the shuttle in case of a mission abort. The ejection induced loading is not structurally significant due to the low 3.5 fps velocity imparted to the satellite by the spring ejection mechanism. Therefore the ejection load was not considered in this thesis. The SSCP program launch limit loads envelope the worst case steady state, low frequency transient, and higher frequency vibroacoustic launch and landing environments. Launch loads vary with each launch and are therefore defined by statistical properties. Limit loads are defined by NASA to be the estimated 97.7 % (2σ) probability of occurrence with 50 % confidence based on a one-sided tolerance limit [Ref. 5]. The launch limit loads for the Hitchhiker/SSCP program are given in Table 1.

Axis	Load Factor (g)	Angular Acceleration $(rad / \sec^2)$
X	± 11	± 85
Y	± 11	± 85
Z	± 11	± 85

Table 1. Hitchhiker Payload Limit Load Factors.

The Hitchhiker program also requires factors of safety on the limit loads due to possible variations in loading and material properties. There are two methods outlined in the Hitchhiker reference guide for the application of factors of safety. The first requires structural testing at 1.25 times the limit loads and analysis showing positive margins of safety at 1.4 times the limit loads for all ultimate failure modes. The second method requires analysis showing positive margins of safety at 2.0 times the limit loads for material yield and 2.6 times the limit loads for ultimate failure modes. This thesis

6

utilized the second method for factors of safety. This will result in a more robust structure and easier qualification on other launch vehicles if desired. The loading utilized in the design and analysis are design loads. The design loads are obtained by multiplying the limit loads by the respective factors of safety. The design loads must be applied simultaneously and in all possible combinations to arrive at the worst case loading condition.

The stiffness constraints imposed by the Hitchhiker program require a fundamental frequency greater than 35 Hz. It is desirable to have the fundamental frequency above 50 Hz. Testing of the natural frequency must be conducted if the predicted value is less than 100 Hz. Verification by finite element math model or classical methods is also required if the predicted frequency falls below 100 Hz. Payloads having a predicted frequency below 50 Hz must submit a test verified finite element math model showing six rigid body frequencies of less than 0.001 Hz. The adapter design constraints made it unlikely that the lowest natural frequency would fall below 100 Hz. However, this thesis utilized a finite element math model to confirm the natural frequencies.

C.   ADAPTER ENVELOPE

The adapter must mate properly with the ejection system (separation plane, pusher plate, and Marman clamp system) and the satellite. The Marman clamp system consists of two semi-circular clamping bands with a keyway in one band. The bands are released during the ejection sequence by squibs allowing the spring loaded pusher plate to eject the satellite. The ejection system requirements leave little room for variation in the shape and size of the adapter. Figure 4 details the overall adapter dimensions, viewing from the separation plane into the satellite. Figures 5, 6, and 7 show the various sections of Figure 4. It is important to note the required shape lines

and the envelope limit lines in Figure 5. The largest driving factor in the design of the adapter is the required envelope.
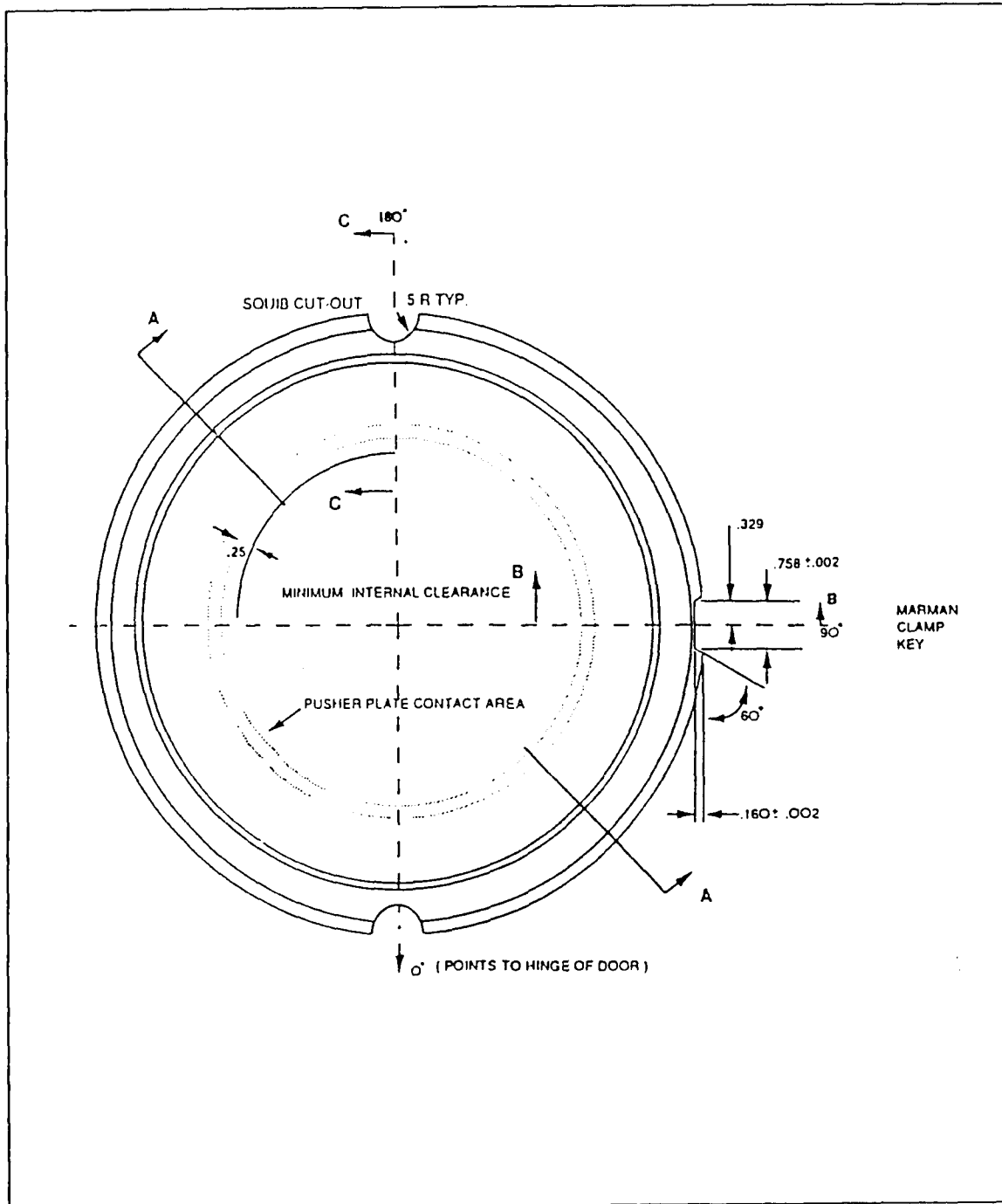
Figure 4. Adapter Envelope Viewed from Separation Plane [Ref. 3].

Figure 5. Section A-A of Adapter Envelope [Ref. 3].

9

.160 REF
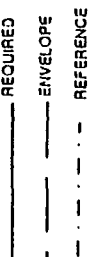
Figure 6. Section B-B of Adapter Envelope [Ref. 3].

2.00 MIN.

1.5 MIN.

1.00 MIN.

Figure 7. Section C-C of Adapter Envelope [Ref. 3].

III. DESIGN TOOLS

The design of the PANSAT adapter must include analysis of both stress and frequency as well as an easily understandable model of the component. Classical methods are difficult to apply in a stress and frequency analysis of a component as 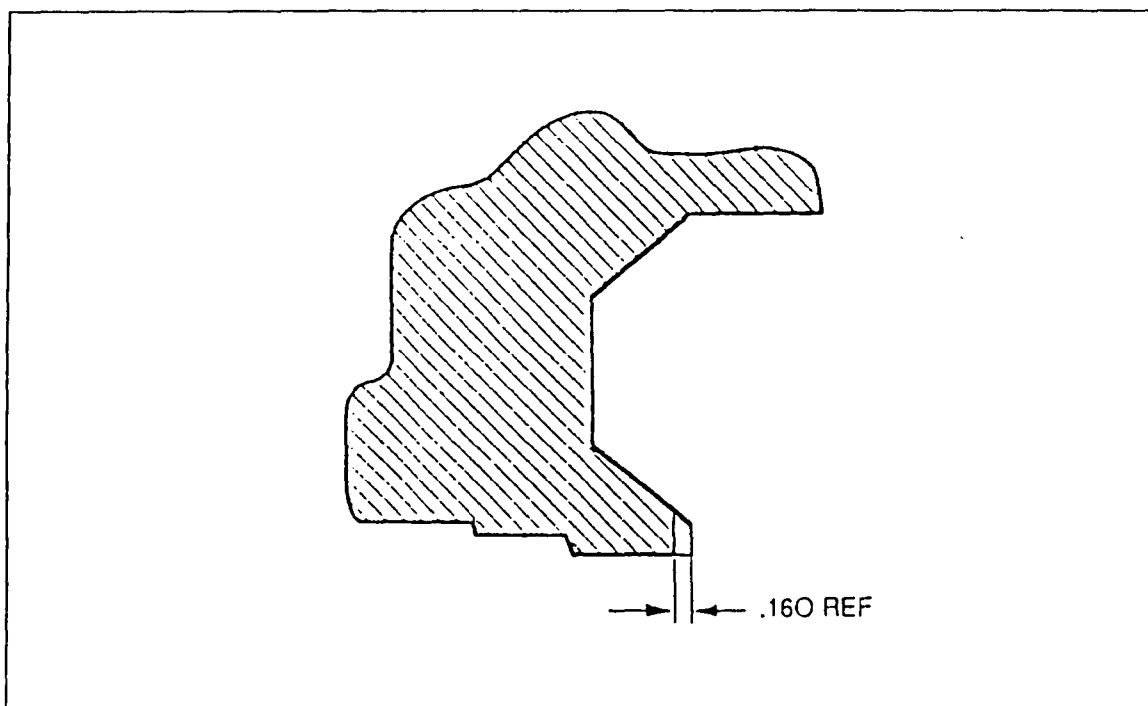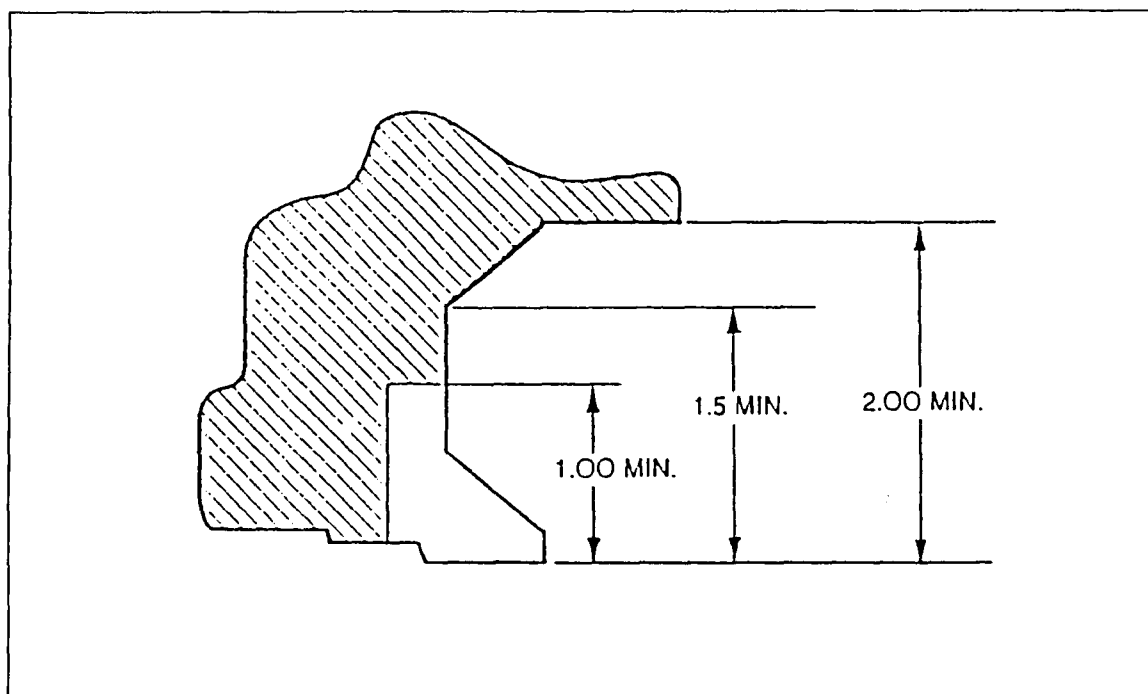complex in shape as the adapter. Computer software was extensively utilized in the design and analysis of the PANSAT adapter.

A.   I-DEAS SOFTWARE

The I-DEAS™ software is a product of the Structural Dynamics Research Corporation (SDRC®). I-DEAS incorporates solid modeling, finite element based stress and frequency analysis and a host of other applications. This software runs on Unix workstations and is not available for personal computers. A large hard disk drive is required as the program itself can consume upwards of 500 MB while model files can easily top 10 MB. Additional space is required for analysis. A large finite element model can generate a hypermatrix file for analysis hundreds of megabytes in size. Run time depends heavily on the number and types of elements and nodes in the model. The run time is a geometric progression, so a small increase in the number of nodes results in a much larger increase in run time. Models of over 5000 nodes can take over an hour to run a stress analysis and over three hours for a frequency analysis. It is also important to remember that a model with a large number of nodes drastically increases the size of the stiffness matrix that must be decomposed and stored in the hypermatrix file, therefore adequate disk space is imperative.

Initial design of a part is accomplished by solid modeling. Two dimensional (2D) drawings are made on a work plane and then constrained, dimensioned and modified as required. The 2D sketch is then extruded into a solid model. This is a true solid model, not a shaded wireframe. Any face of the solid model can be sketched on and extruded in constructing the part. Boundary conditions are added to the completed part to simulate loads, pressures, and restraints. A finite element model is then generated utilizing 1D, 2D, or 3D elements and checked for distortion and stretch. The elements can be corrected by a number of methods to prevent errors in the solution. The elements reference the material properties for the material assigned to the part. A solution set is then created and the model solved for stress, natural frequency or a number of other results. The part can be easily resized to lower stress, raise the natural frequency, or reduce deflection for example. Another analysis can be run without deleting the mesh or boundary conditions. Most of the features in the software are automatic, for example, finite element meshes can be generated automatically and need only be approved by the operator. This software makes development of parts and assemblies a much smoother operation, reducing time and costs significantly. A number of major manufacturers (Lockheed, GE, and Mitsubishi for example) currently utilize this product while the trend among manufacturers is to increase the use of CAD/CAM programs to remain competitive.

B. MATHCAD

MATHCAD® is a mathematical calculation program for personal computers. This program allows a wide range of technical calculations with equations, text and graphics. Equations are typed just as they would appear hand written. Mathcad solves the equations numerically or symbolically,

graphs the results if desired, and can be linked to another application like a word processor. Complex operations like differentiation, integration, solving for a variable, or computing a Taylor Series can be accomplished. Units follow through the entire set of calculations. Arrays or matrices of large size can be solved. Numerous uses exist for this software, from the classroom to the practicing engineer.

IV. STRUCTURAL DESIGN

The adapter fitting design is driven by several factors which must be prioritized. The biggest factor and first on the priority list is to ensure the adapter fitting is within the available envelope. Strength, stiffness, and stability are next in priority. The PANSAT project was conceived as a low cost satellite, therefore the adapter cost is next in priority. Lastly, the weight of the adapter is considered. PANSAT is allowed a total weight of 150 lbf. The current estimate for total weight falls far below this limit. Orbit predictions for PANSAT show that the greater the weight of the satellite, the longer it will remain in orbit due to the effects of aerodynamic drag [Ref. 6]. Thus weight is a low priority for the adapter fitting.

A.   ADAPTER

The adapter dimensions about the separation plane and Marman clamp area are fixed by the adapter envelope requirements, so that the adapter will mate properly with the clamping mechanism. The areas that are open for design flexibility are above the Marman clamp and in the center of the adapter volume. The maximum height for the entire satellite (including the adapter fitting) is 20.5 in to fit within the GAS canister. The center of mass of the satellite is limited to a maximum of 10.25 in above the separation plane to limit bending loads on the Marman clamp assembly. A low center of mass results in reduced bending loads on the adapter. The adapter height was set at 2.00 in, the minimum allowed by the envelope requirements, to reduce bending loads and to lower the center of mass of the satellite.

15

The maximum adapter diameter is 9.375 in at the separation plane. This extends horizontally beyond the edges of the bottom panel of PANSAT, overlapping the lower angled panels. The overlapping results in shadowing the solar cells mounted on the lower angled panels when the sun orientation is below the adapter as shown in Figure 8.
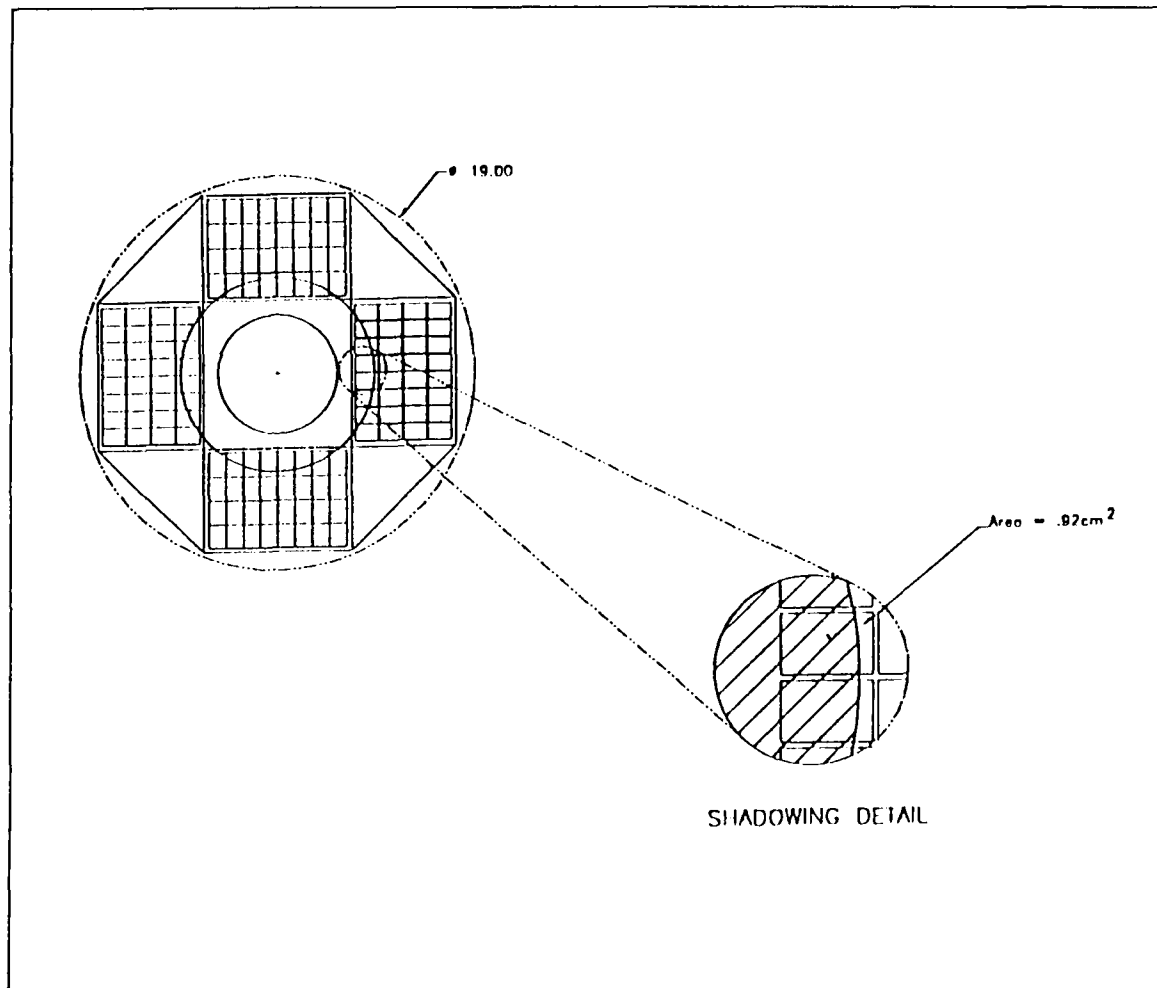

Figure 8. Adapter Shadowing Pattern [Ref. 1].

Since PANSAT has no attitude control, this orientation is likely to occur often and will reduce power output from the solar array. The power margin of the satellite may or may not be able to absorb this loss, therefore an adapter design option that does not shadow the solar cells is desirable. Removal of

16

the material on the adapter that will shadow the solar array will drastically reduce the clamping surfaces mating with the Marman clamp assembly, driving the clamp pressures significantly higher in order to prevent separation during launch. The Marman clamp assembly preload limits are not known. Since the Marman clamp will not be engaged on its entire surface in a non-shadowing adapter design, two options are presented in this thesis for a shadowing and a non-shadowing design.

The material choices for the adapter are limited by several design requirements: high strength, high elastic modulus, low density, good machinability, low cost, and good availability. Material properties must come from MIL-HDBK-5D [Ref. 4]. High technology composite materials were not considered in this design due to the expense and manufacturing difficulties presented by these materials.

The first design option for the adapter is a shadowing version. The full lower envelope is utilized, engaging the entire Marman clamp assembly. The design tapers to a circular profile at the top to reduce weight and fit within the bottom panel of PANSAT. The central portion of the adapter is hollowed out to reduce weight as well. The material chosen for this option is 6061-T651 aluminum plate since the expected loads are not high and the material is cheap and easy to manufacture [Ref. 7]. The solid model for the first option is shown in Figure 9. There are two squib cutouts and one keyway cutout on the perimeter of the adapter. The thickness of material at the top of the adapter was kept to 0.8125 in so as to leave enough material for through fastener holes. This option does shadow the solar cell arrays when the sun orientation is directly below the adapter. This could be a major drawback to the operation of the satellite. Since the satellite will tumble on orbit, this orientation could occur frequently and significantly lower the power output of the illuminated arrays. However, since the final power margin has yet to be determined, this design was fully analyzed as a viable option.
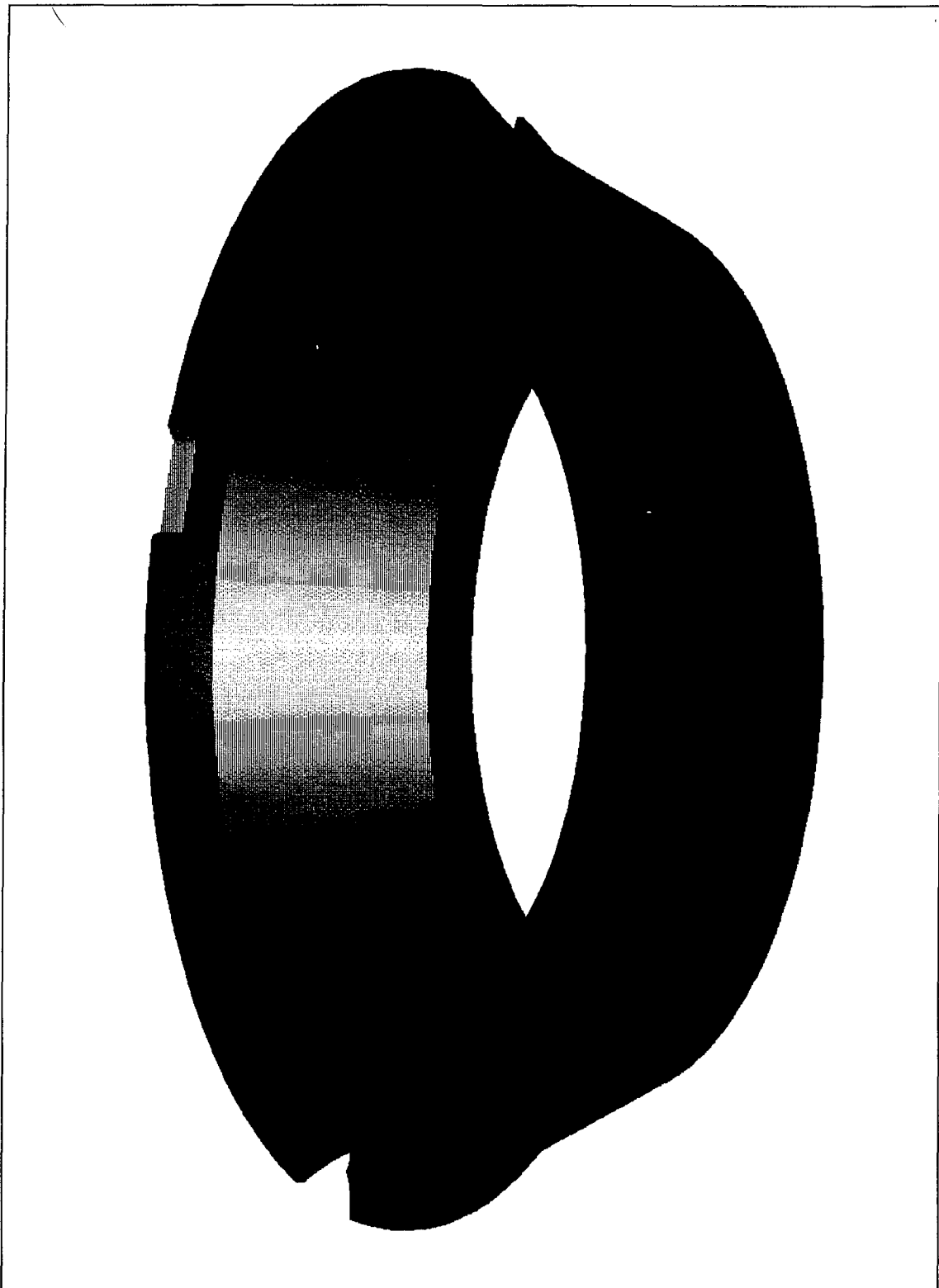
Figure 9. Solid Model for Adapter Option One.

Because the first design could detrimentally affect the solar array, a second, non-shadowing option was desired. The second design option utilizes the same profile as the first but has one significant difference. The sides of the design were cut vertically, in line with the perimeter of the bottom panel of PANSAT. This removes all the material that could shadow the lower arrays when the sun is directly below the adapter. The difficulty arises in the clamping surface remaining for the Marman clamp assembly. The remaining clamping surface is aproximately 15 % of that available in the first option design. Since the clamping surface is small, the clamping pressure required to keep the adapter firmly against the separation plane during launch increases dramatically. There also is less area to support the loads developed during launch. The stresses developed from the clamping pressure and launch loads will be much higher than those in the first design. Composites and beryllium were ruled out due to the expense and manufacturing problems associated with these materials. · Therefore a titanium beta alloy (Ti-13V-11Cr-3Al) was chosen for design option two. Ti-13V-11Cr-3Al is a much stronger and stiffer material than 6061 aluminum and can be machined with carbide tipped tooling relatively easily [Ref. 7]. Figure 10 shows the solid model for the second design option. Note the lack of squib cutouts or a keyway in the solid model of Figure 10. The sqiubs and keyway will be located on the flat sides of the model where the is no contact with the Marmon clamp. This provides more than adequate room for the sqiubs but no adapter interaction with the Marmon clamp key. At the time of this thesis, it was unclear whether a keyway was required. However, the significantly higher clamping pressure combined with even a low coefficient of friction should prevent the adapter from rotating within the clamp assembly during launch. Therefore a keyway is unnecessary in this design. Results of detailed analysis on both adapter design options are presented in Chapter V.

19
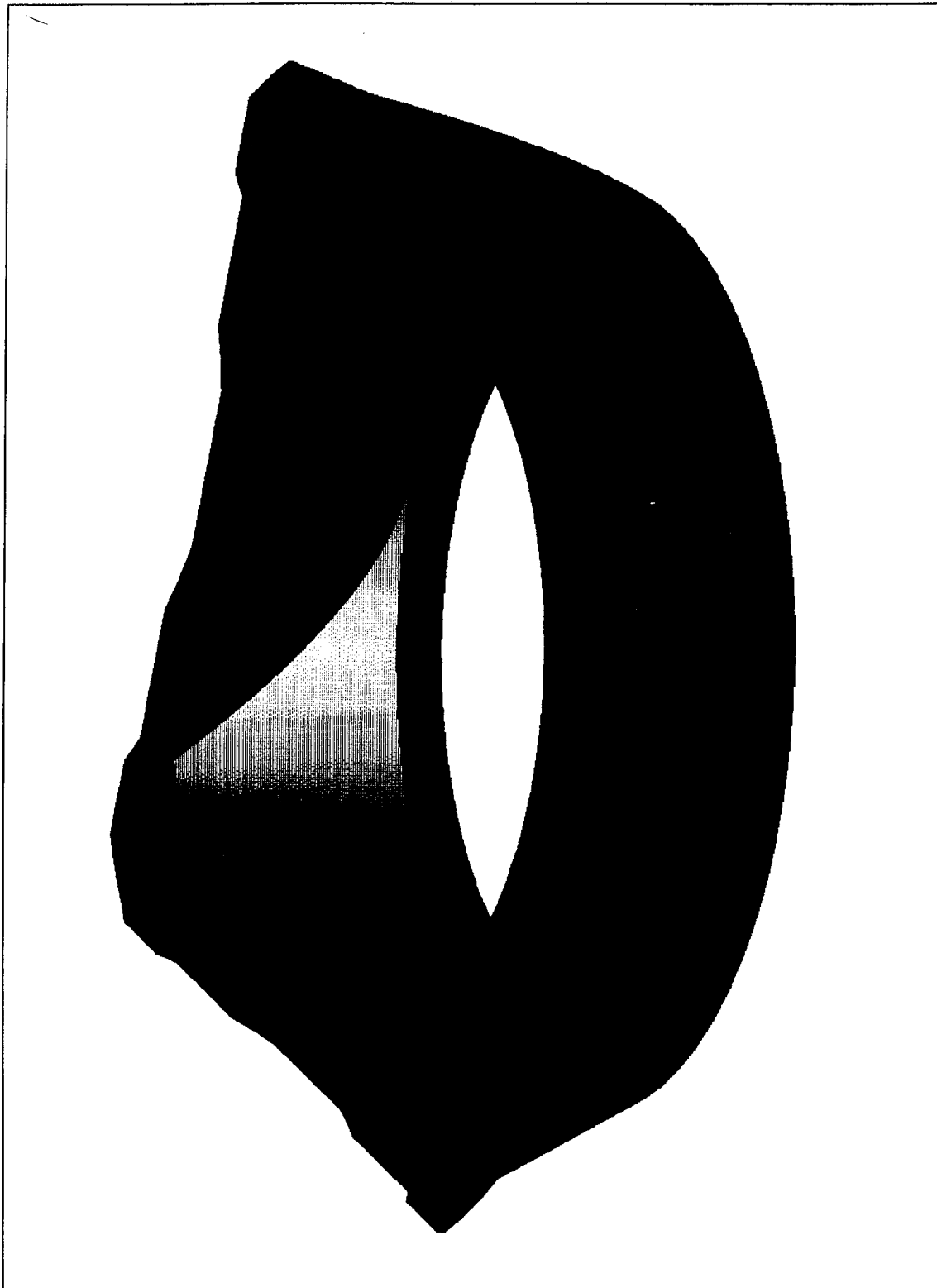
Figure 10. Solid Model for Adapter Option Two.

B. FASTENERS

The adapter requires some method to affix it to the bottom panel of PANSAT. Welding has been used to join parts utilized for space applications before but it requires a meticulous quality control process with extensive documentation, inspection, and testing, particularly for manned launch vehicles. Therefore, fasteners will be used to join the adapter to PANSAT. Accessibility and ease of assembly were given high priority in the fastener design. The method chosen passes the fasteners through the adapter, bottom panel, and flange with a nut to secure the threaded end of the fastener. This method requires less disassembly to remove the adapter from PANSAT since a nut is much easier to maneuver in the confined interior of the satellite. The fastener heads require countersinks in the bottom of the adapter fitting so as not to protrude beyond the adapter envelope and possibly interfere with the pusher plate.

There are numerous types and sizes of commercially available fasteners to choose from, not to mention custom made items. The fastener design only considered standard fastener sizes for cost and availability reasons [Ref. 8]. The fastener pattern consists of eight fasteners arranged in a circular pattern about the center axis of the adapter top surface. The pattern radius was pushed out as far as possible to reduce the loading on the individual fasteners. Proper sizing of the fasteners required considering the loading and adapter material remaining about the fastener holes. The fastener tensile area must be large enough to carry the preload and the launch loads, but also small enough to prevent shear tearout. Two design options were also cosidered for the fasteners. The first option uses 1/4-28 UNF PH13-8Mo-H1000 stainless steel fasteners [Ref. 7]. These standard size fasteners have high strength and are commonly available. The second uses 5/16-24 UNF Ti-6Al-4V titanium alloy fasteners [Ref. 7]. These standard fasteners were chosen for high strength and material compatability. Both

21

fastener options are commonly used in space applications. Results of detailed analysis on both fastener design options are presented in Chapter V.

V. FINITE ELEMENT MODELING AND ANALYSIS

A.   ADAPTER

The two adapter design options were subjected to detailed analysis for stability, strength, and frequency. A buckling analysis was completed utilizing classical methods while the finite element method was used to determine maximum Von Mises stress and the lowest natural frequency.

1.   Buckling Analysis

A cylindrical shell under compression from an axial or bending load can be subject to elastic instability. Buckling of the shell can occur if the applied stress is equal or greater than the critical stress for buckling. The critical stress for an axial compressive load is

$$\sigma_c = \gamma \frac{E}{\sqrt{3(1-v^2)}} \frac{t}{r} \tag{1}$$

$$\gamma = 1 - 0.9\left(1 - e^{-\phi}\right) \tag{2}$$

$$\phi = \frac{1}{16}\sqrt{\frac{r}{t}} \quad , \quad \text{for} \quad \left(\frac{r}{t} < 1500\right) \tag{3}$$

where σ_c is the critical stress, E the elastic modulus, v is Poisson's ratio, r is the radius, and t is the thickness of the walls. The critical stress for bending load is the same as that for axial compression except for the correlation factor as shown below

$$\gamma = 1 - 0.731\left(1 - e^{-\phi}\right) \tag{4}$$

23

The margin of safety for buckling is given by

$$M.S. = \frac{1}{R_c + R_b} - 1 \qquad (5)$$

$$R_c = \frac{\sigma_{axial}}{\sigma_c} \qquad (6)$$

$$R_b = \frac{\sigma_{bending}}{\sigma_b} \qquad (7)$$

where *M.S.* is the margin of safety, and σ_{axial}, $\sigma_{bending}$, are the actual stresses due to the axial load and bending load respectively. [Ref. 5]

It is imperative to have large critical buckling stresses, preferably well above the yield and ultimate strengths of the material, for a sucessful design. Due to the complex geometry of both adapter options, the critical buckling stresses were calculated using a simplified geometry. The geometry was assumed to be a cylinder with a radius of 3.5625 in, wall thickness of 0.8125 in, and height of 2.00 in. This produces critical buckling stresses lower than would be expected from either design, and therefore would eliminate further analysis if the adapter options met the design requirements. The critical buckling stresses for both adapter designs are given in Table 2.

Adapter Option	Compression Stress (psi)	Bending Stress (psi)
Aluminum Alloy	891,712	911,212
Titanium Alloy	1,396,116	1,426,646

Table 2. Critical Buckling Stress Results.

The results show that the critical buckling stresses are far above the yield and ultimate strengths of the adapter materials. Therefore, buckling is not a failure mode of concern for the adapter design options and further buckling analysis is not required.

2. Finite Element Analysis

Finite element analysis breaks a component up into a number of small pieces or elements to approximate the infinite number of points available in a given component. Elements can be one, two, or three dimensional as required by the complexity of the component. Seemingly complex components can often be modeled by simpler two or one dimensional elemnts with a coresponding reduction in computation time. Elements are created by connecting nodes, forming the edges of the element. The greater the number of nodes available in an element, the more degress of freedom for that element. Each element is constrained by boundary conditions at its nodes by interaction with an adjacent element, external restraints, loads, constraints, or a free end for example.

I-DEAS uses the displacement based finite element method to solve finite element models. The principal of virtual work is used to derive the equilibrium equations as follows

$$\int_V \{\hat{\varepsilon}\}^T \{\sigma\} dV = \{\hat{U}_i\}^T \{F_i\} + \int_S \{\hat{U}\}^T \{f_s\} dS + \int_V \{\hat{U}\}^T \{f_B\} dV \qquad (8)$$

where
$\{\hat{U}\} =$ virtual displacement

$\{\hat{\varepsilon}\} =$ strain due to the virtual displacement

$\{\sigma\} =$ actual stress at current time t due to applied loads

$\{F_i\} =$ nodal forces

$\{f_s\} =$ surface forces

$\{f_B\} =$ body forces

The left hand side represents the internal strain energy due to the virtual displacement integrated over the volume. The right hand side represents the external work due to point loads, surface loads, and body forces. A set of continous element interpolation functions $\{N\}$ and their derivatives $\{B\}$ are introduced to evaluate the forces and displacements at any place in the body from a set of nodal values. The virtual displacement vector is cancelled from the previous equation leaving

$$\sum_{elem\,V_e} \int [B]^T \{\sigma\} dV_e = \{F_i\} + \sum_{elem\,S_e} \int [N]^T \{f_S\} dS_e + \sum_{elem\,V_e} \int [N]^T \{f_B\} dV_e \qquad (9)$$

with the integrals computed over each element and summed to form a global set of equations. The linear case simplfies for the displacement, $\{u\}$, to the familiar form

$$[K]\{u\} = \{F_i\} + \{F_S\} + \{F_B\} \qquad (10)$$

where linear stiffness matrix, $[K]$, is computed from

$$[K] = \sum_{elem\,V_e} \int [B]^T [D][B] dV_e \qquad (11)$$

and $[D]$ is the matrix of elastic constants. The linear relations

$$\{\varepsilon\} = [B]\{u\} \qquad (12)$$

$$\{\sigma\} = [D]\{\varepsilon\} \qquad (13)$$

are used to recover strain and stress as secondary quantities. [Ref. 9]
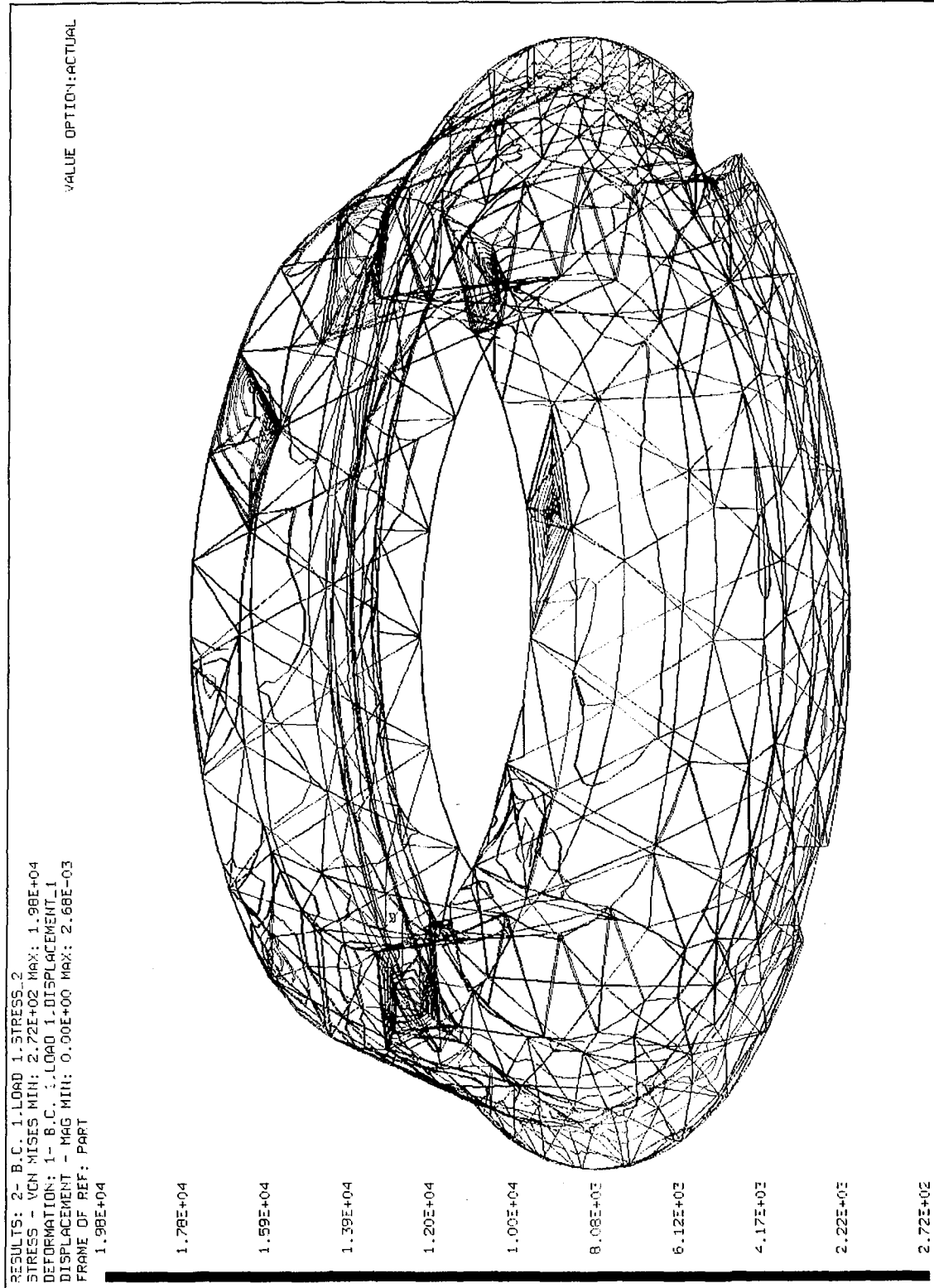
a. Stress Analysis

There are several options available in the full I-DEAS software package for three dimensional elements. However, element choices were limited to tetrahedrons and parabolic tetrahedrons due to the less comprehensive software package installed at the Naval Postgraduate School.

26

Parabolic tetrahedrons were used because, due to the addition of mid-nodes, they have a lower inherent stiffness than standard tetrahedrons. The finite element analysis was run as an iterative process. The finite element mesh was increased in density for each iteration to approach convergence in the solution. The final iteration for adapter option one used a finite element mesh of 5714 nodes and 3192 elements while adapter option two used 5530 nodes and 3167 elements. Computation time for the final iteration of each adapter design exceeded two hours and taxed the limits of available disk space for hypermatrix files.

The launch loads can combine into 64 different loading conditions, of which the worst case was applied to the finite element models. However, the loading due to the Marman clamp was undefined in the Hitchhiker program requirements. Assumed Marman clamp loads were computed through a static analysis for the pressure required to restrain each adapter option against the separation plane under worst case launch loads. The pressures were calculated at 1618 psi for adapter option one and 16,330 psi for adapter option two. The critical stress areas occur in the vicinity of the Marman clamp for each adapter option.

The worst case loading used in the finite element analysis included the factor of safety of 2.6 for ultimate strength. The increase in factor of safety from yield to ultimate results in an increase in applied stress of 30 %, while the increase in material strength from yield to ultimate is only 16.22 % for adapter option one and 6.25 % for adapter option two. If the adapter designs show positive margins of safety for ultimate strength, they will be even more positive for yield strength, therefore the worst case loading condition occurs with the ultimate strength factor of safety. Figures 11 and 12 show the finite element analysis stress profiles for adapter options one and two respectively. The results of the finite element analysis at the critical stress area of each adapter option are shown in Table 3.

Figure 11. Stress Profile for Adapter Option One.

RESULTS: 2- B.C. 1 LOAD 1.STRESS_2
STRESS - VON MISES MIN: 2.72E+02 MAX: 1.98E+04
DEFORMATION: 1- B.C. 1.LOAD 1.DISPLACEMENT_1
DISPLACEMENT - MAG MIN: 0.00E+00 MAX: 2.68E-03
FRAME OF REF: PART

VALUE OPTION:ACTUAL

1.98E+04

1.78E+04

1.59E+04

1.39E+04

1.20E+04

1.00E+04

8.08E+03

6.12E+03

4.17E+03

2.22E+03

2.72E+02

RESULTS: 2- B.C._1,LOAD_1,STRESS_2
STRESS - VON MISES M'N: 4.02E+02 MAX: 7.54E+04
DEFORMATION: 1- B.C._1,LOAD_1,DISPLACEMENT_1
DISPLACEMENT - MAG MIN: 0.00E+00 MAX: 3.44E-03
FRAME OF REF: PART

VALUE OPTION:ACTUAL

7.54E+04

6.79E+04

6.04E+04

5.29E+04

4.54E+04

3.79E+04

3.04E+04

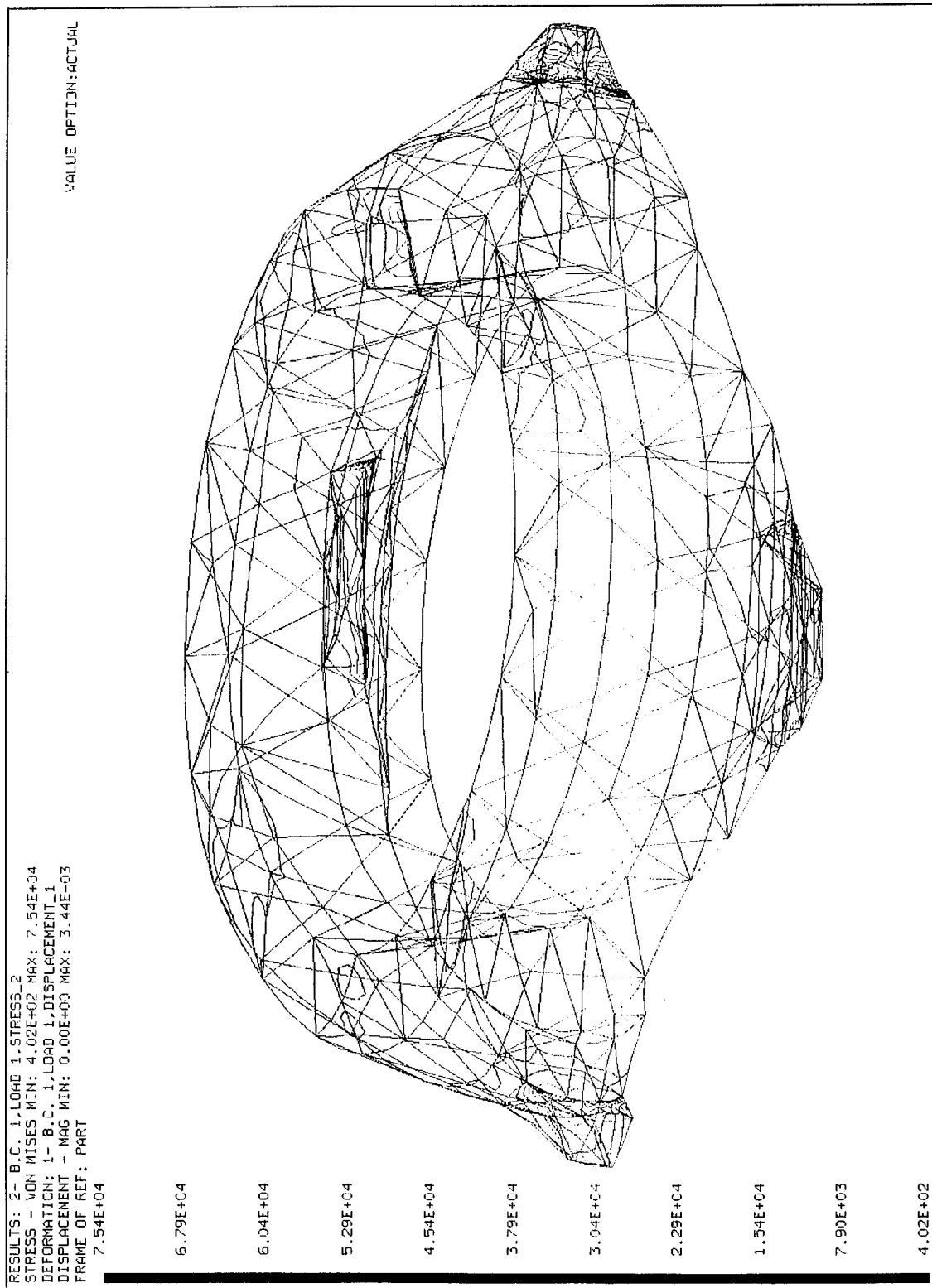2.29E+04

1.54E+04

7.90E+03

4.02E+02

Figure 12. Stress Profile for Adapter Option Two.

29

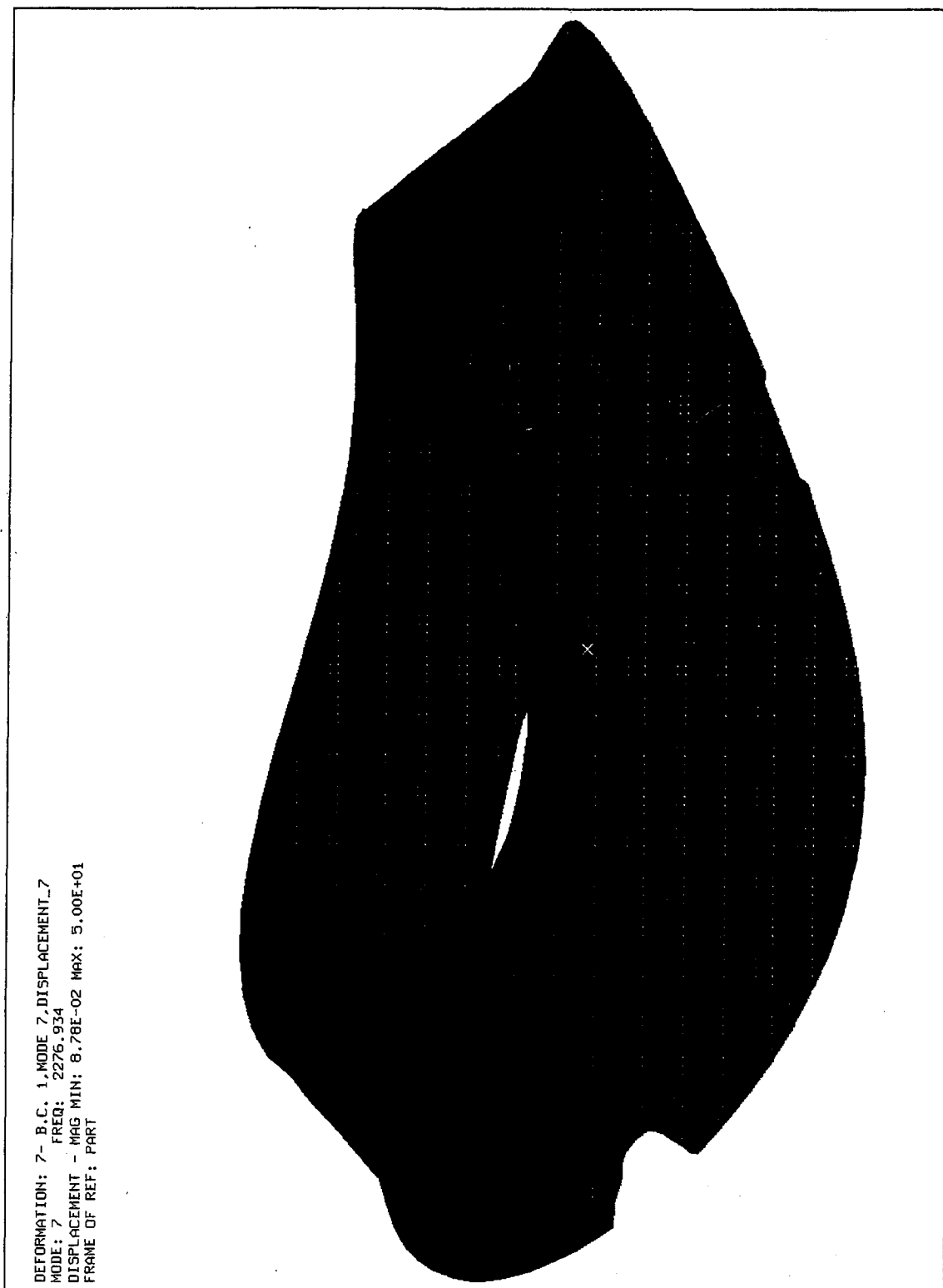| Adapter Option	Ultimate Material Strength (psi)	Applied Stress (FS of 2.6 included) (psi)	Margin of Safety
Aluminum Alloy	43,000	14,285	2.01
Titanium Alloy	170,000	75,427	2.25

Table 3. Stress Results for Adapter Design Options.

The results show that both adapter design options show positive margins of safety, under worst case loading, and exceed the design specifications.

b. *Frequency Analysis*

Frequency analysis takes far more computation time and produces far larger hypermatrix files than stress analysis. The finite element models used in the final iteration of the stress analysis were used for the frequency analysis but the computations ran for three hours before running out of disk space. The density of the mesh for both models was then reduced to prevent the hypermatrix file from exceeding available disk space. The reduced mesh density produced 2684 nodes and 1386 elements for adapter option one with 1328 nodes and 625 elements for adapter option two. The models were unrestrained in the frequency analysis but a frequency shift of 1 Hz was applied to remove singularities. The computation time with the reduced mesh density still exceeded two hours.

The results of the analysis showed the lowest natural frequency for adapter option one was 2276 Hz while that for adapter option two was 1925 Hz. The results are not unexpected since both options have no long, thin profiles that would produce low natural frequencies. Both adapter options exceed the Hitchhiker design specifications. The lowest natural frequency modes are shown in Figures 13 and 14 for adapter option one and two respectively.

DEFORMATION: 7- B.C. 1,MODE 7,DISPLACEMENT_7
MODE: 7   FREQ: 2276.934
DISPLACEMENT - MAG MIN: 8.78E-02 MAX: 5.00E+01
FRAME OF REF: PART

Figure 13. Lowest Natural Frequency Mode for Adapter Option One.

31

Figure 14. Lowest Natural Frequency Mode for Adapter Option Two.

DEFORMATION: 7- B.C. 1,MODE 7,DISPLACEMENT_7
MODE: 7   FREQ: 1925.814
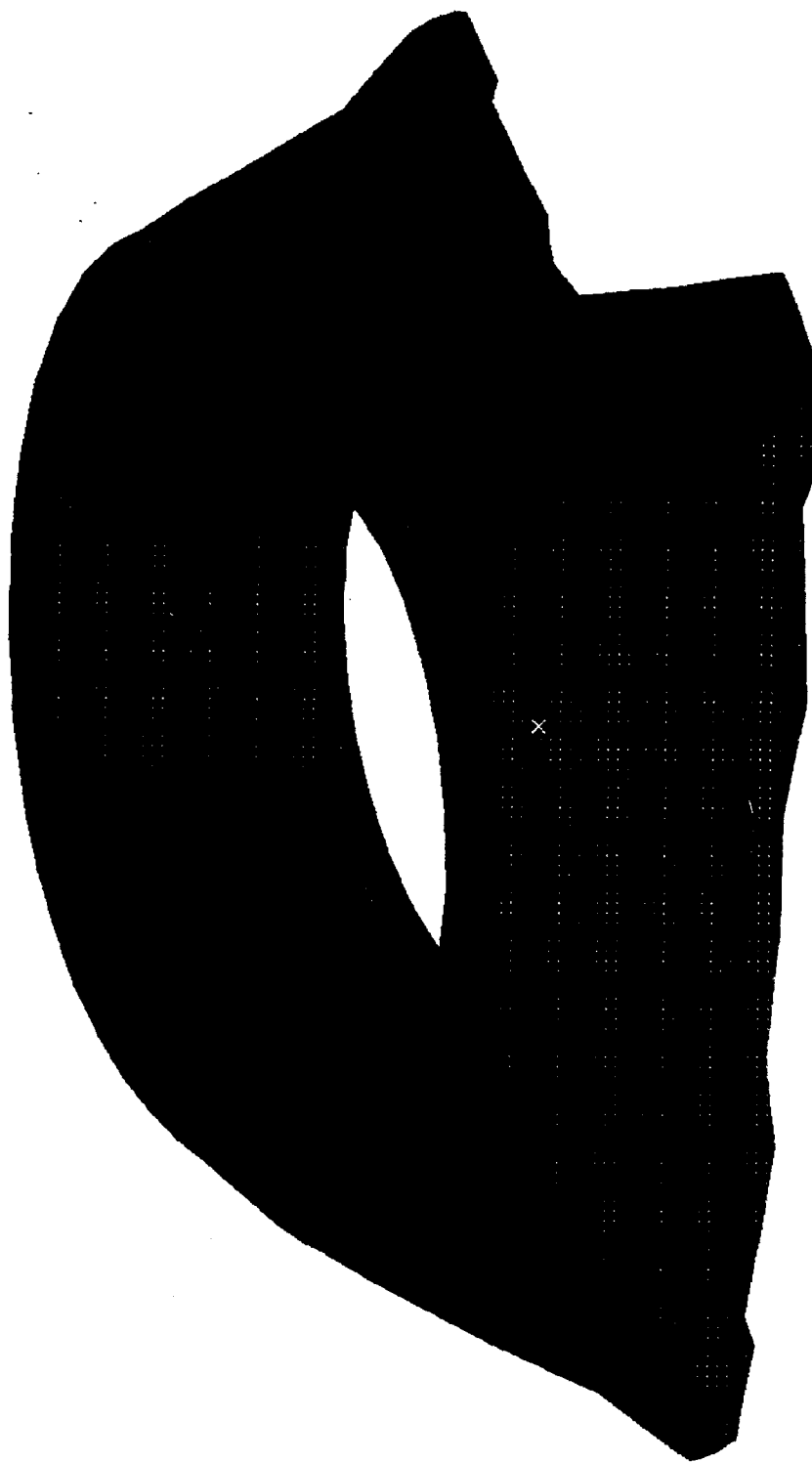DISPLACEMENT - MAG MIN: 7.50E-01 MAX: 3.94E+01
FRAME OF REF: PART

All design specifications were exceeded by both adapter design options. Adapter option two is recommended for use on PANSAT since it will not shadow the solar cells when the sun orientation is directly below the adapter. This will cost more in materials and labor but it will enable PANSAT to meet mission requirements without drastic operational limitations from low power output of the solar cells.

B. FASTENERS

1. Preload Calculation

The two fastener design options were analyzed using classical fastener methods for preload and Von Mises stress [Ref 10,11]. The fasteners and material clamped between them can be thought of as springs with some stiffness value associated with them. This technique assumes that in the absence of external load, the fastener and parts when assembled (or preloaded) are deflected to different degrees by the same preload. The fastener is deflected in tension, and the parts are deflected in compression. When an external load is then applied, the fastener and the parts are then constrained to deflect by the same magnitude. A properly designed joint will have the characteristic of expending the majority of the external load in uncompressing the joined parts, while the fastener extends very little. The fastener stiffness should be lower than the stiffness of the joined parts to take advantage of this effect. The stiffness for each component of the bolted connection is

$$k = \frac{AE}{L} \tag{14}$$

where A is the area, E is the elastic modulus, and L is the length of the component. The fastener is normally made up of a shank and a threaded

portion, which have individual stiffnesses. These are combined into the overall fastener stiffness

$$\frac{1}{k_b} = \frac{1}{k_s} + \frac{1}{k_t} \tag{15}$$

where k_b is the fastener stiffness, k_s the shank stiffness, and k_t the threaded stiffness. The joined material stiffness, k_m, is calculated by combining the individual part stiffnesses in a similar manner, while the areas used depend on the geometry of the parts as shown in Figure 15.
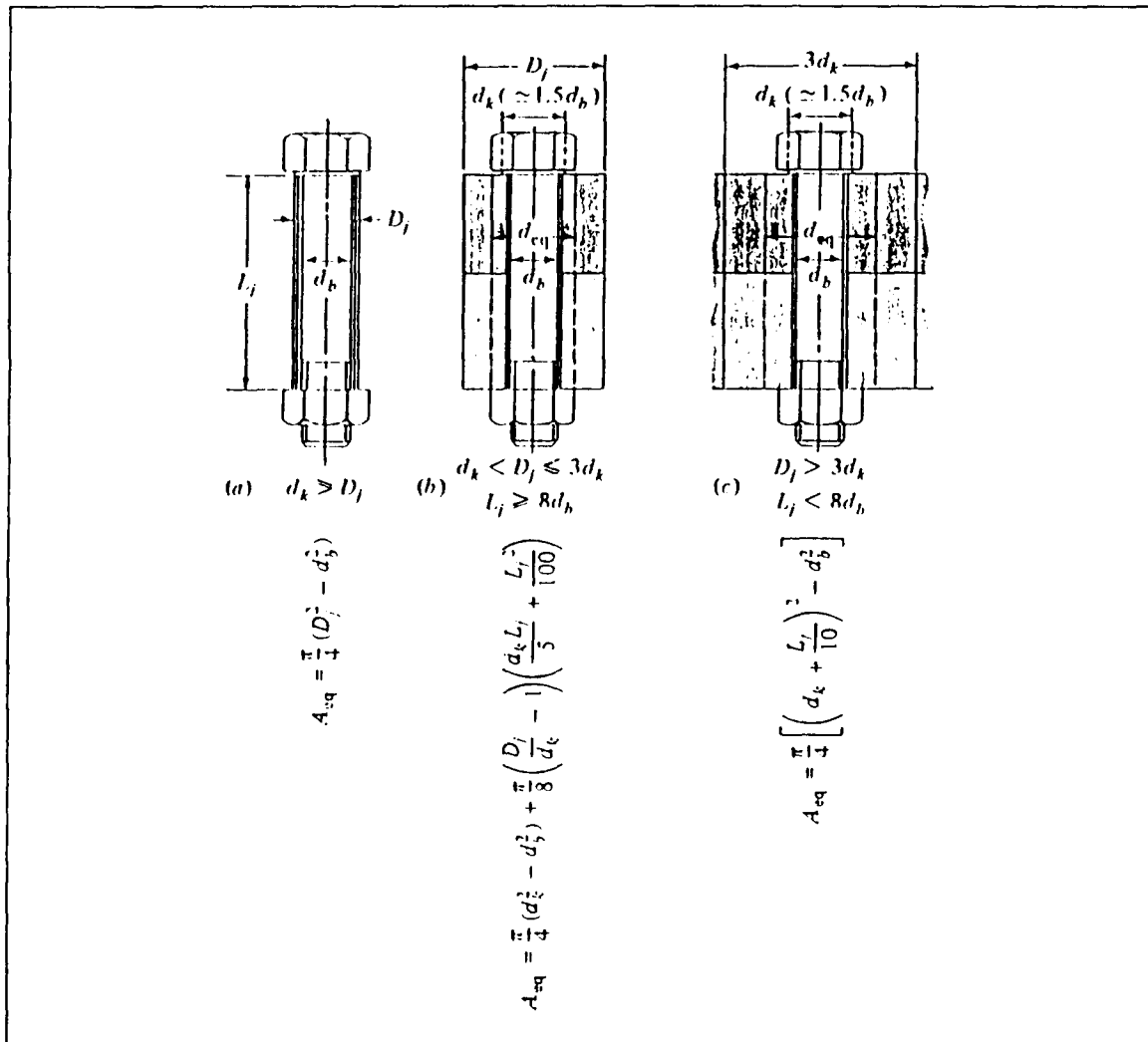

Figure 15. Joint Component Stiffness [Ref. 10].

34

The force on the fastener can then be calculated from

$$F_b = F_i + CP \qquad (16)$$

and,

$$C = \frac{k_b}{k_b + k_m} \qquad (17)$$

where F_b is the force on the bolt, F_i the preload, and P the external load. The minimum preload to prevent separation of the joined components is calculated by setting the fastener force F_b equal to the external load P and solving for the preload.

The worst case launch loading condition was assumed in calculating the fastener preloads, and a safety margin of 10 % was added to the results for variations in loading and material properties. The minimum preloads calculated for both fastener design options are shown in Table 4.

Fastener Option	Preload for Adapter Option 1 (lbf)	Preload for Adapter Option 2 (lbf)
Stainless Steel	2619	2982
Titanium Alloy	2926	3249

Table 4. Preload Results for Fastener Design Options.

2. Stress Analysis

The principal stresses were calculated using the above preloads and the worst case tensile loading condition. The launch loads on the fasteners were simplified into a plane stress problem. The resultant loading condition contained only one tensile and shear load. Principal stresses are calculated from

$$\sigma_{max,min} = \frac{F_{tensile}}{2 \cdot A} \pm \sqrt{\left(\frac{F_{tensile}}{2 \cdot A}\right)^2 + \left(\frac{F_{shear}}{A}\right)^2} \qquad (18)$$

where $\sigma_{max,min}$ are the maximum and minimum principal stresses respectively, $F_{tensile}$ is the tensile load, F_{shear} is the shear load, and A is the load carrying area of the fastener. Failure criteria must be applied to properly evaluate fastener performance. The maximum Von Mises stress failure criteria is frequently used for ductile materials and provides a somewhat conservative failure envelope. The Von Mises stress is calculated by

$$\sigma = \frac{1}{\sqrt{2}} \cdot \left[(\sigma_1 - \sigma_2)^2 + (\sigma_1 - \sigma_3)^2 + (\sigma_2 - \sigma_3)^2\right]^{\frac{1}{2}} \qquad (19)$$

where $\sigma_1 = \sigma_{max}$, $\sigma_2 = 0$, and $\sigma_3 = \sigma_{min}$ for a plane stress condition. The maximum Von Mises was combined with the material yield and ultimate strengths to produce margins of safety for the fasteners options. The margins of safety are shown in Tables 5 and 6.

Adapter Option	Margin of Safety Yield	Margin of Safety Ultimate
Aluminum Alloy	0.504	0.466
Titanium Alloy	0.475	0.458

Table 5. Margins of Safety for Stainless Steel Fasteners.

Adapter Option	Margin of Safety Yield	Margin of Safety Ultimate
Aluminum Alloy	0.479	0.437
Titanium Alloy	0.455	0.431

Table 6. Margins of Safety for Titanium Alloy Fasteners.

The results show that both fastener options have positive margins of safety for yield and ultimate strengths and thus satisfy the SSCP design specifications. The stainless steel option is recommended for PANSAT use due to the higher margins of safety. Stainless steel fasteners are also more readily available and lower in cost.

VI. CONCLUSIONS

The finite element method is extremely useful in solving complex problems not readily solvable by classical means. The I-DEAS software used was very comprehensive in the types of problems that can be solved. The solid modeling aspect is very useful in visualizing the component and would be extremely helpful in assembly by showing tolerance errors and assembly overlaps. The software must be used frequently to gain proficiency but the wealth of online help makes questions on software operation easy to answer.

The design process is an attempt to optimize the performance of a component with respect to the design specifications. The specifications for the PANSAT adapter were somewhat inflexible with respect to adapter size and shape but open in choice of materials. Loading conditions were severe due to the requirements of a manned mission. The effects of the design on the entire system must also be taken into account. The effect of the adapter on the satellite system was recognized and shaped adapter option two so that the solar cells would not be shadowed. Fasteners were also considered with the design effect on assembly given a high priority. All design options for the adapter and fasteners exceeded the Hitchhiker program specifications and would perform the adapter mission well on PANSAT. However, the final choice on design must keep systems engineering in mind. The design recommended for PANSAT is the titanium alloy adapter (adapter option two) combined with stainless steel fasteners (fastener option one). This choice will allow excellent performance of the adapter component without detrimentally affecting the performance of the entire satellite.

Further work on the adapter is recommended in the areas of testing and system analysis. The accuracy of the finite element model can be verified through structural testing of the component for strength and

stiffness. The entire satellite structure can be modeled with finite elements and analyzed for natural frequency modes while restrained by the Marman clamp assembly. Stress distributions could be obtained from a more realistic loading condition using launch accelerations on each element of the structure and equipment placement represented by lumped masses.

LIST OF REFERENCES

1. Sakoda, D.J., *Effective Area of a Tumbling PANSAT for Solar Power Flux*, SSAG-D-PA003, Space Systems Academic Group, Naval Postgraduate School, Monterey, CA, April 1994.

2. Sakoda, D.J., *Structural Design, Analysis, and Modal Testing of the Petite Amateur Navy Satellite (PANSAT)*, Master's Thesis, Naval Postgraduate School, Monterey, CA, September 1992.

3. *Get Away Special Ejection System User Handbook*, Preliminary, National Aeronautics and Space Administration, October 1989.

4. *Hitchhiker Customer Accommodations & Requirements Specifications*, HHG-730-1503-06, National Aeronautics and Space Administration, Goddard Space Flight Center, 1992.

5. Agrawal, B.N., *Design of Geosynchronous Spacecraft*, Prentice-Hall Inc., Englewood Cliffs, NJ, 1986.

6. Cuff, D.J., *Lifetime and Reentry Prediction for the Petite Amateur Navy Satellite (PANSAT)*, Master's Thesis, Naval Postgraduate School, Monterey, CA, June 1994.

7. *Metallic Materials and Elements for Areospace Vehicle Structures*, MIL-HDBK-5E, Department of Defense, May 1986.

8. Avallone, E.A., and Baumeister, T., *Mark's Standard Handbook for Mechanical Engineers*, Ninth Edition, McGraw-Hill Inc., New York, NY, 1987.

9. I-DEAS Software On-Line Help Database, *Understanding the Linear Statics Formulation*, Structural Dynamics Research Corporation, 1993.

10. Edwards, K.S., and McKee, R.B., *Fundamentals of Mechanical Component Design*, McGraw-Hill Inc., New York, NY, 1991.

11. Shigley, J.E., and Mischke, C.R., *Mechanical Engineering Design*, Fifth Edition, McGraw-Hill Inc., New York, NY, 1989.

INITIAL DISTRIBUTION LIST

		No. Copies
1.	Defense Technical Information Center Cameron Station Alexandria VA 22301-6145	2
2.	Library, Code 052 Naval Postgraduate School Monterey CA 93943-5002	2
3.	Dr. Rudolph Panholzer Chairman, Space Systems Academic Group Code SP Naval Postgraduate School Monterey CA 93943-5002	1
4.	Dr. Daniel J. Collins Chairman, Aeronautics and Astronautic Department Code AA Naval Postgraduate School Monterey CA 93943-5002	1
5.	Dr. Sandra L. Scrivener Code AA/SS Naval Postgraduate School Monterey CA 93943-5002	6
6.	Dr. I. Michael Ross Code AA/RO Naval Postgraduate School Monterey CA 93943-5002	1
7.	Mr. Daniel J. Sakoda Code SP/Sd Naval Postgraduate School Monterey CA 93943-5002	1

8.   LT. Brian B. Gannon   4
      Naval Surface Warfare Center
      Port Hueneme Division
      Code 4A00
      4363 Missile Way
      Port Hueneme CA 93043-4307